spectra did not change either when they were recorded rotating the cuvette 90° around the light axis or after strong cuvette shaking. Moreover, rectangular cuvettes of 0.5 cm and a 1-cm optical path were used, which exclude the alignments of mesophases that thin cuvettes can cause. In this sense, the chirality previously detected in cyanine dye J-aggregates was later rejected on the basis of LD artifacts [see cited references in (*18*)]. However, recent reports [e.g., (*10*)] on similar J-aggregates have excluded LD contributions with similar experimental cautions to those reported here. We detected dichroic signals due to these artifacts in the case of solutions containing very large aggregates, but these solutions were obtained under different experimental conditions. Finally, we found that because of resonance light scattering effects at the absorption bands of these homoassociates (*31*), differential scattering may be an important contribution to the CD spectra (*32*), but such contributions are also related to the molecular chirality (*33*).

16. This was observed for the ORD spectra recorded in a Pockel's cell instrument as well as for those obtained in a calcite prisms instrument.
17. Two important questions are worth remarking on at this point: (i) the UV/vis absorption bands of the homoassociates occur at very different wavelengths than those of the monomeric species (*11–13*), allowing us to attribute unambiguously the detected chirality to the homoassociate chromophores; (ii) the huge absorptivity of the porphyrin chromophor transitions results in high rotational strengths and leads to high sensitivities in the detection of enantiomeric excesses.
18. M. Avalos *et al.*, *Chem. Rev.* **98**, 2391 (1998).
19. True chirality meets the nonexchange condition between enantiomers through the space reversal as well as with the time reversal operators (e.g., a vortex translation). False chirality meets this condition through the space reversal operator (e.g., rotation in a gravitational field) [(*18*); L. D. Barron, *Chem. Soc. Rev.* **15**, 189 (1986)].
20. In fact, complementary experiments conducted with magnetically stirred solutions where aggregation was suddenly fostered by acidification of a free base porphyrin solution, at near to constant ionic strength, did not show any substantial signature of chiral selection.
21. G. Bersuker, *J. Chem. Phys.* **110**, 10907 (1999).
22. N. Harada, K. Nakanishi, *Circular Dichroism Spectroscopy. Exciton Coupling in Organic Spectroscopy* (University Science Books, Mill Valley, CA, 1983).
23. P. J. Collings *et al.*, *J. Phys. Chem. B* **103**, 8474 (1999).
24. K. Misawa, T. Kobayashi, *J. Chem. Phys.* **110**, 5844 (1999).
25. O. Katzenelson, H. Z. Hel-Or, D. Avnir, *Chem. Eur. J.* **2**, 174 (1996).
26. B. L. Feringa, R. A. van Delden, *Angew. Chem. Int. Ed.* **38**, 3419 (1999).
27. C. Girard, H. B. Kagan, *Angew. Chem. Int. Ed.* **37**, 2922 (1998).
28. J. M. Seddon, R. H. Templer, in *Handbook of Biological Physics*, R. Lipowsky *et al.*, Eds. (Elsevier Science, New York, 1995), vol. 1, pp. 97–160.
29. S. F. Mason, *Nature* **311**, 19 (1984).
30. V. Avetisov, V. Goldanskii, *Proc. Natl. Acad. Sci. U.S.A.* **93**, 11435 (1996).
31. R. F. Pasternack, P. J. Collings, *Science* **269**, 935 (1995).
32. R. Rubires, J.-A. Farrera, J. M. Ribó, *Chem. Eur. J.* **7**, 436 (2001).
33. C. Bustamante, I. Tinoco Jr., M. F. Maestre, *Proc. Natl. Acad. Sci. U.S.A.* **80**, 3568 (1983).
34. Supported by DGI (Spanish Government) and CUR (Generalitat de Catalunya).

19 March 2001; accepted 19 April 2001

Modulation of Cell Proliferation by Heterotrimeric G Protein in *Arabidopsis*

Hemayet Ullah,[1] Jin-Gui Chen,[1] Jeff C. Young,[2]* Kyung-Hoan Im,[1] Michael R. Sussman,[2] Alan M. Jones[1]†

The α subunit of a prototypical heterotrimeric GTP-binding protein (G protein), which is encoded by a single gene (*GPA1*) in *Arabidopsis*, is a modulator of plant cell proliferation. *gpa1* null mutants have reduced cell division in aerial tissues throughout development. Inducible overexpression of *GPA1* in *Arabidopsis* confers inducible ectopic cell division. *GPA1* overexpression in synchronized BY-2 cells causes premature advance of the nuclear cycle and the premature appearance of a division wall. Results from loss of function and ectopic expression and activation of *GPA1* indicate that this subunit is a positive modulator of cell division in plants.

Heterotrimeric G proteins regulate cell growth, differentiation, and transformation in animal cells (*1*). Many growth factors activate receptors that transmit signals to the cytoplasm through heterotrimeric G proteins. Of the 17 Gα subunits that have been cloned, 10 couple mitogenic signaling (*2*, *3*). Studies of the interaction between Gα subunits and proliferation support the emerging view that the α subunits form a new class of oncogenes (*4–6*).

[1]Department of Biology, University of North Carolina at Chapel Hill, Chapel Hill, NC 27599, USA. [2]Cell and Molecular Biology Program and the Department of Horticulture, University of Wisconsin, 1575 Linden Drive, Madison, WI 53706, USA.

*Present address: Biology Department, MS-9160, Western Washington University, Bellingham, WA 98225, USA.

†To whom correspondence should be addressed at Department of Biology, CB#3280, University of North Carolina at Chapel Hill, Chapel Hill, NC 27599–3280, USA. E-mail: alan_jones@unc.edu

The *Arabidopsis* genome contains a single prototypical Gα (*GPA1*) gene, offering a unique advantage over its animal counterparts to dissect its role in cell proliferation. Various signals such as auxin, cytokinin, brassinosteroids, light, sucrose, stress, and developmental factors modulate cell proliferation in plants as well (*7*). On the basis of *GPA1* expression in actively dividing cells, it has been suggested that GPA1 is involved in promoting active cell division (*8*), a notion supported by the observation that a rice Gα mutant confers a dwarf phenotype (*9*).

By screening an *Arabidopsis* transferred DNA (T-DNA) insertion population (*10*), two recessive mutant alleles, *gpa1-1* and *gpa1-2*, were identified and shown by direct sequencing to harbor T-DNA in the predicted seventh intron (*gpa1-1*) and in the eighth exon (*gpa1-2*) (Fig. 1A). Northern hybridization results showed the expected size of truncated mutant transcripts (Fig. 1C) and that the steady-state levels of the mutant transcripts were not affected in the dark. The insertion eliminates four of its five polypeptide loops required for GTP binding (*11*), the guanosine triphosphatase (GTPase) domain, and the effector loop. On the basis of parallel structure-function studies on animal Gα, the *Arabidopsis* GPA1 mutant proteins are predicted to be nonfunctioning. Western hybridization with antiserum directed against a recombinant *Arabidopsis* GPA1 showed that, in the mutant lines, no Gα protein of any size was detected. This indicates that the T-DNA insertions in both *gpa1-1* and *gpa1-2* produce null alleles or that the truncated gene product is no longer recognizable by the antibodies to GPA1 (Fig. 1D).

gpa1 mutants displayed phenotypes that were consistent with a reduction in cell division throughout development, although with contrasting effects on organ morphogenesis. In light-grown seedlings, *gpa1* leaf size and morphology were maintained despite fewer cells composing this organ. Compensation by increased cell size for reduced cell number during organ morphogenesis has been documented frequently (*12–14*), supporting the theory that the individual cell is not always the basic unit of morphogenesis in plants. However, *gpa1* mutants also illustrate that a reduction of cell number results in reduced hypocotyl length, providing the alternative example of morphogenesis.

Exposure of wild-type plants to light marks the start of photomorphogenic development called de-etiolation. Both *gpa1* mutant alleles displayed partial de-etiolation (Fig. 2). Dark-grown *gpa1* mutant seedlings had short hypocotyls and open hooks typical of light-irradiated seedlings, but the root and cotyledon phenotypes were dark-grown wild type (WT). Scanning electron microscopy revealed that the constitutive hook opening is due to the normal expansion of adaxial cells

of the *gpa1-1* mutant (Fig. 2, compare C and D).

The short hypocotyl of *gpa1* seedlings was due to a reduced number of elongating cells (Fig. 3), indicating impaired cell division. *gpa1* mutants have about 10 hypocotyl cells (Fig. 3A), compared with the typical 20 cells of the WT (Fig. 3B). The number of hypocotyl cells is established during embryogenesis, whereas hypocotyl length after germination is established almost exclusively by cell elongation (*15*). Maximum cell lengths in *gpa1* mutants were normal, and no additional compensating cells were observed in the hook region (Fig. 2C).

Normal leaf morphogenesis is driven by cell division and expansion. Division begins at the apex of the primordium and moves basipetally ahead of a wave of cell expansion to drive the major increase in leaf area. Additional cell divisions within intercalary meristems influence leaf shape. Epidermal leaf cells of 3-week-old *gpa1* mutants are significantly larger and fewer at all positions examined in the leaf (Fig. 3E). This increase in cell expansion compensates the reduction in cell division in the *gpa1* mutants. The *gpa1* mutants exhibit a *rotundifolia*-like (*16*) leaf shape when grown in light (Fig. 3C). *Rotundifolia* encodes cytochrome P450, which might be involved in brassinosteroid synthesis (*17*). We have found that *gpa1* mutants have reduced brassinolide responsiveness (*18*), consistent with the phenotype of *rotundifolia*.

To visualize the deduced decrease in cell division, we analyzed a mitotic reporter (*19*, *20*) in the *gpa1* background. β-Glucuronidase (GUS) staining of both the apical meristems and basal cells of the first leaf was markedly reduced in *gpa1* mutants compared with controls (Fig. 4). Because overall leaf expansion was slightly faster in *gpa1* seedlings, comparisons were made to wild-type seedlings that were both developmentally (5-day-old) and chronologically (4-day-old) the same as *gpa1* expanding leaves. Although the normal basal pattern of division in the control leaves was apparent as a discrete and intense wave of staining, this pattern was not observed in developing *gpa1* leaves. Instead, weak and diffuse GUS staining in aerial tissues was consistently found. The most likely explanation of this result is that G_1 of the nuclear cycle is lengthened in *gpa1* cells. As expected, owing to a lack of a root phenotype, GUS staining in *gpa1* roots was consistently similar to GUS staining in WS roots, indicating that Gα does not regulate proliferation in root meristems. Therefore, we view Gα as an intermediate signal element integrating signals that modulate cell division. Signals modulating division are necessarily different between root and shoot cell types (*21*).

Inducible, ectopic expression of *GPA1* in *Arabidopsis* conferred inducible, ectopic cell division in multiple organs. Three homozygous lines transformed with *GPA1* under the control of a dexamethasone (dex)-inducible promoter showed distinctive phenotypes only after exposure to dex, whereas control plants did not display a dex-dependent phenotype (Fig. 5). The induced phenotypes showed medium to severe reduction in growth (Fig. 5, B and C) that correlated with the level of

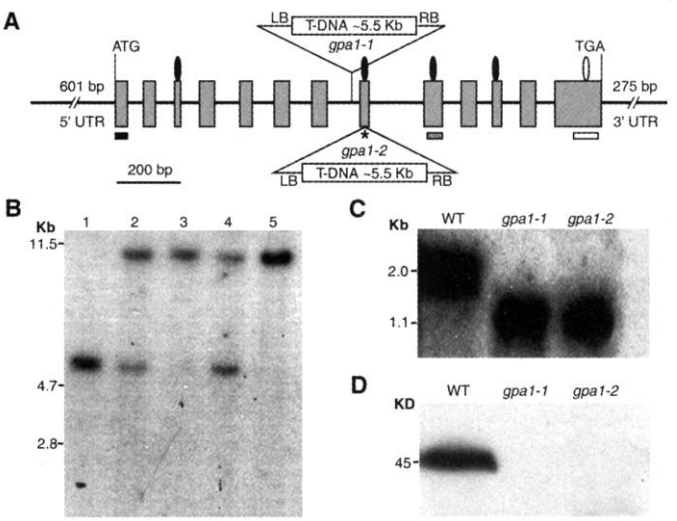

Fig. 1. *GPA1* insertion mutants. (**A**) T-DNA insertion sites in *GPA1*. LB, T-DNA left border; RB, T-DNA right border. Gray vertical boxes represent exons. The binding domain for the G_β and G_γ subunits is indicated by the horizontal black box at the NH_2-terminus. Black ovals above exons indicate the position of the polypeptide loops for GTP binding. The white oval is the putative fifth loop for GTP binding. The white horizontal box at the COOH-terminus represents the position of the putative receptor interaction domain. The asterisk represents Switch 1 of the GTPase domain, and the effector loop. The horizontal hatched box is Switch II. The T-DNA insert is not drawn to scale. Bar, 200 base pairs (bp). (**B**) Southern blot analysis with a genomic polymerase chain reaction product generated from the 3′ region of *GPA1*. The indicated lanes contain 10 μg of Spe I–digested genomic DNA from wild-type seedlings (lane 1), and seedlings heterozygous at *gpa1-1* (lane 2), homozygous at *gpa1-1* (lane 3), heterozygous at *gpa1-2* (lane 4), and homozygous at *gpa1-2* (lane 5). (**C**) Northern blot analysis. The indicated lanes contain 20 μg of total RNA from WT (lane 1), *gpa1-1* (lane 2), and *gpa1-2* (lane 3) plants grown for 2 days in dark. A *GPA1* cDNA (*8*) was used as hybridization probe. The mutants show truncated transcripts, as expected from their T-DNA insertion site. (**D**) Immunoblot analysis. Membrane proteins (20 μg) were extracted from 1-week-old, dark-grown seedlings as indicated and subjected to immunoblot analysis with a polyclonal antiserum against recombinant GPA1 as described (*32*).

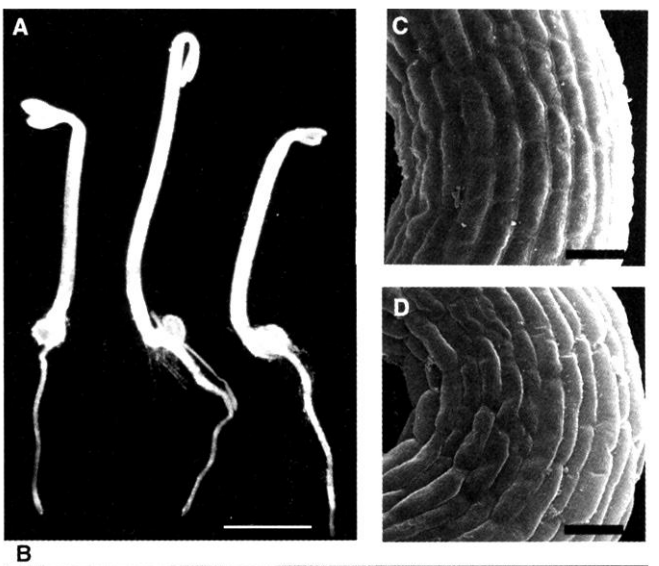

	Hypocotyl length (mm)	Degrees of hook opening	Root length (mm)	Cotyledon area (μm² X 1000)
WT	5.9 +/- 0.35	18 +/- 4.0	3.43 +/- 0.14	17.90 +/- 1.01
gpa1-1	3.1 +/- 0.46	88 +/- 17.0	3.67 +/- 0.18	17.08 +/- 1.19
gpa1-2	2.8 +/- 0.39	92 +/- 11.0	3.84 +/- 0.12	17.27 +/- 0.65

Fig. 2. (**A**) Morphology of wild-type, and mutant, 2-day-old seedlings. Wild-type and mutant seedlings were grown in the dark for 2 days on 0.5× MS salts (pH 5.7), 0.8% agar, 1% sucrose plates. Wild type (middle), *gpa1-1* (left), and *gpa1-2* (right). Bar, 1.5 mm. (**B**) Effect of T-DNA insertion on the hypocotyl and root length, degree of hook opening, and cotyledon area. Standard error of the mean is based on a minimum of 10 seedlings. Closed hooks were treated as having zero degree of opening. (**C** and **D**) Scanning electron micrograph at the hook region of *gpa1-1* (C) and wild type (D). Bar, 25 μm.

GPA1 expression. Each phenotype could be explained by ectopic cell division. This is most evident in the shoot epidermis, where ectopic division planes and decreased cell area in leaves overexpressing *GPA1* are abundant (Fig. 5, H to K). Furthermore, overexpression of *GPA1* led to excessive cell division in meristematic regions, as well as initiation of adventitious meristems (Fig. 5D).

To determine more precisely how GPA1 modulates cell division, we expressed *Arabidopsis GPA1* in synchronized tobacco BY-2 cells (line designated GOX1). The DNA content was measured in synchronized cells 6 hours later, after cells were released from aphidicolin-induced arrest [Web fig. 1, A and B (*22*)]. The addition of auxin shifts the percentage of control cells in G_2 from 15 to 60% during this time; however, synchronized GOX1 cells advance to the maximum G_2 percentage in the absence of auxin. Furthermore, whereas synchronized control cells had not synthesized a cell plate 24 hours after release from aphidicolin inhibition, 50% of GOX1 cells showed a nascent cell plate during this time [Web fig. 1, C and D (*22*)]. The auxin-induced advance in nuclear cycle was also demonstrated by increased [^{3}H]thymidine incorporation in control cells [Web fig. 1E (*22*)]. The results indicate that overexpression of *GPA1* leads to increased cell division by shortening G_1, consistent with the lengthened G_1 phase predicted by the behavior of the loss-of function mutants. Additional support for a role for GPA1 in modulating cell division is shown with the use of Mas7, an activator of Gα. The addition of Mas7, but not the inactive analog Mas17, markedly increased DNA synthesis in control cells, consistent with the *Arabidopsis* and BY-2 *GPA1* overexpression data [Web fig. 1 (*22*)].

In mammals, the βγ subunit of heterotrimeric G proteins also triggers cell proliferation, but indirectly, by way of the mitogen-activated protein kinase (MAPK) pathway (*1*, *2*, *23*–*25*). Because Gβγ does not change conformation upon binding to Gα (*26*, *27*), its downstream actions are solely dependent on Gα activation and subsequent dissociation of the heterotrimeric complex (*24*). One interpretation of the current results is that a plant Gβ modulates cell division because activation of Gα releases sequestration of Gβγ subunits in the cell. Therefore, a possible consequence of Gα overexpression could manifest its phenotype on a MAPK pathway regulated by the Gβγ subunits. Signal transduction by auxin, a prominent modulator of plant cell division and elongation, appears to use a MAPK pathway. Activation of the MAPK cascade suppresses auxin signal transduction (*28*), and therefore the partial inhibition of cell division in *gpa1* plants might result from Gβγ suppression of a

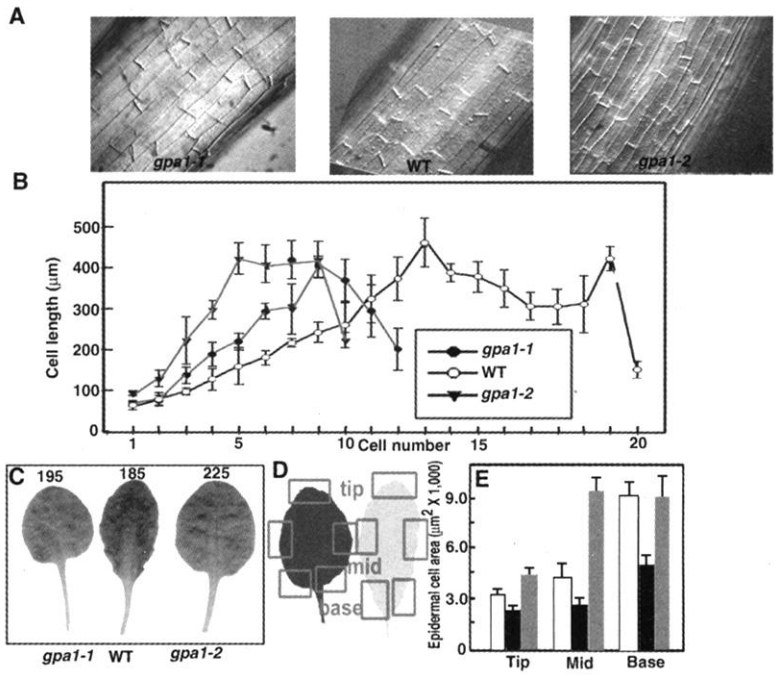

Fig. 3. Reduced cell division in developing hypocotyls and leaves. (**A**) Hypocotyl cell sizes of WT (WS ecotype) and *gpa1* mutants grown for 2 days in the dark. Seedlings were cleared in chloral hydrate and observed by Nomarski microscopy. (**B**) Cell size as a function of the position along the hypocotyls as shown in (A) were measured with NIH Image 1.61 software. (**C**) Light phenotype of 3-week-old WT and *gpa1* mutant leaves. Numbers above the panel indicate the leaf area (in mm^2). (**D**) Schematic diagram showing leaf positions used to measure cell sizes. (**E**) Average cell sizes from areas indicated in (D) measured as described for (B) with epidermal peel of 3-week-old leaves. Open bar, *gpa1-1*; black bar, WT; gray bar, *gpa1-2*. Error bars represent the SEM of size using at least 50 nypocotyl (B) and epidermal (E) cells from six plants.

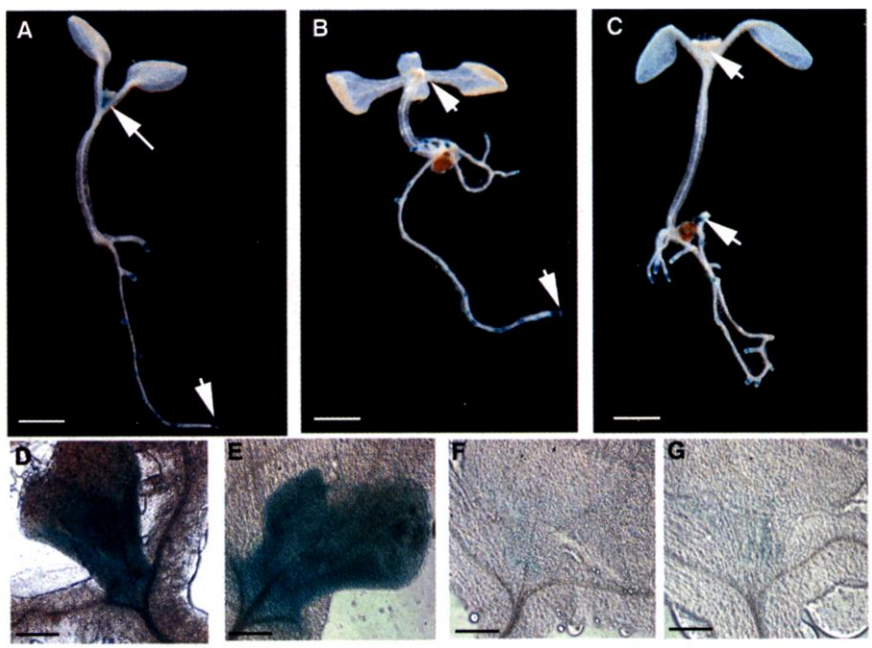

Fig. 4. Histochemical staining showing GUS activity in WT and *gpa1* plants containing the mitotic reporter cyc1At-CDB-GUS. (**A**) WT cyc1At-CDB-GUS plants. (**B**) cyc1At-CDB-GUS plants in *gpa1-1* background. (**C**) cyc1At-CDBGUS plants in *gpa1-2* background. Bar (A to C), 1 mm. Dark-grown seedlings (A to C) are 4 days old. Arrows indicate the first leaf and apical root and shoot meristems. (**D** and **E**) Higher magnification of meristem and expanding leaf of a 4-day-old (D) and 5-day-old WT (E) cyc1At-CDB-GUS. (**F**) *gpa1-1*, 2-day-old plant shown in (B). (**G**) *gpa1-2*, 2-day-old plant shown in (C). Bar (D to G), 10 μm.

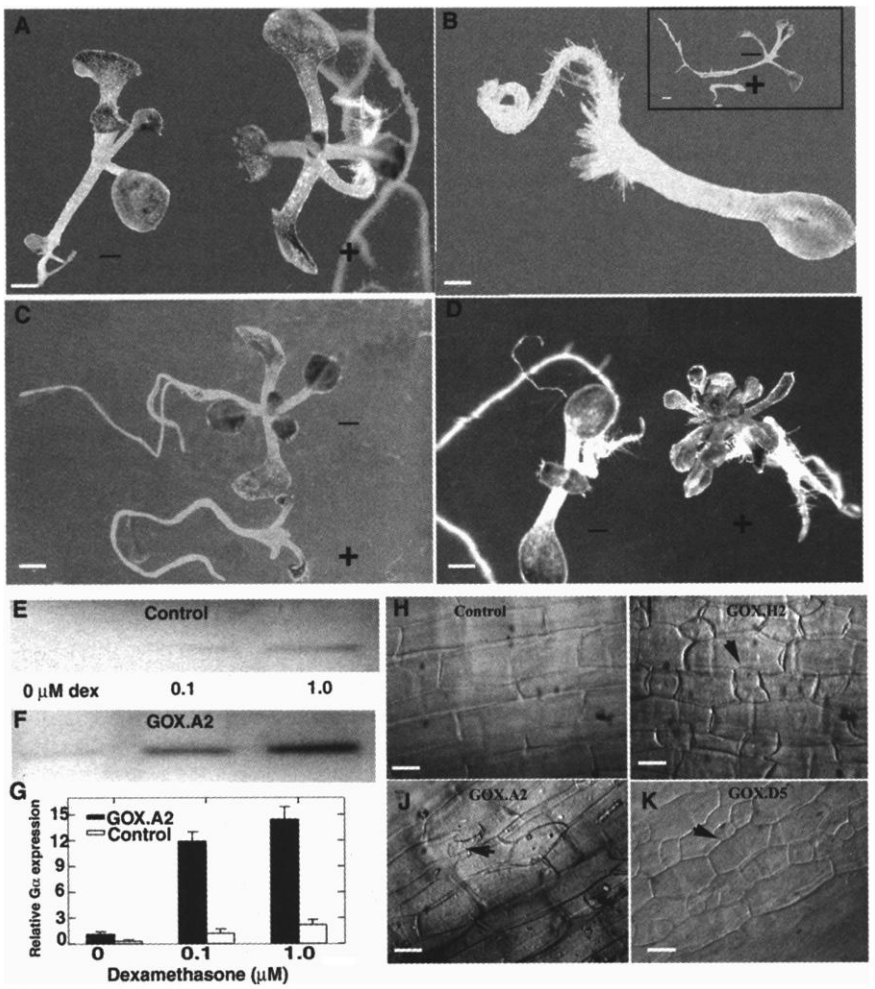

Fig. 5. Dex-dependent phenotypes of seedlings overexpressing *GPA1* (GOX). (**A**) WS ecotype control seedlings grown for 7 days under continuous light with (+) 1 μM dexamethasone (dex) or without dex (−). (**B**) Seedling from GOX.H2 line overexpressing *GPA1* grown with 1 μM dex. (**Inset**) Seedlings from GOX.H2 line grown with (+) or without dex (−). (**C**) Line GOX.A2 overexpressing *GPA1* shows intermediate phenotype. (**D**) Line GOX.D5 overexpressing *GPA1* produces multiple meristems. Bar (A to D), 1 mm. Immunoblot analysis of GPA1 in membrane fractions from control (**E**) and GOX.A2 lines (**F**), grown for 7 days in light with the indicated amount of dex. (**G**) Relative expression level of GPA1 normalized to a nonspecific band. Error bars represent the SEM of pixels from the bands of two independent blots quantitated by the Molecular Dynamics software. (**H** to **K**) Cellular phenotypes from the ectopic expression of *GPA1* induced by 1 μM dex. Bar (H to K), 20 μm. Arrowheads indicate the position of ectopic cell divisions. Transformed lines (H to K) are indicated.

MAPK pathway. Additionally, it is plausible that Gβγ release regulates a potassium channel, as shown for brain cell GIRK2 (*29*).

Cell division and elongation are fundamental cellular processes in the life cycle of plants. Stimuli from multiple signaling pathways become integrated at some point to modulate proliferation. Because *gpa1* mutants are compromised in multiple signal transduction, GPA1 represents this point of integration for many signals. For example, ABA regulation of ion channels in guard cells is completely eliminated (*30*). In addition to the indirect evidence that auxin signal transduction uses GPA1, we find that *gpa1* mutants are less sensitive to gibberellic acid, brassinolide, and ACC and are hypersensitive to sugars. Intuitively, multiple signaling inputs are expected to modulate a single (or few) critical pathway(s) involved in cell division and elongation in plants. Now that a critical player in the cell proliferation pathways has been identified, further studies should clarify the mechanism through which it acts and how it integrates different signaling pathways leading toward cell proliferation.

References and Notes

1. J. S. Gutkind, *J. Biol. Chem.* **273**, 1839 (1998).
2. N. Dhanasekaran, S.-T. Tsim, J. M. Dermott, D. Onesime, *Oncogene* **17**, 1383 (1998).
3. L. A. Selbie, S. J. Hill, *Trends Pharmacol. Sci.* **19**, 89 (1998)
4. N. Dhanasekaran, L. E. Heasley, G. L. Johnson, *Endocr. Rev.* **16**, 259 (1995).
5. D. C. Watkins, G. L. Johnson, C. C. Malbon, *Science* **258**, 1373 (1992).
6. V. J. LaMorte, P. K. Goldsmith, A. M. Spiegel, J. L. Meinkoth, J. R. Feramisco, *J. Biol. Chem.* **267**, 691 (1992).
7. D. Francis, D. Dudits, D. Inze, Eds., *Plant Cell Division* (Portland Press Research Monograph, London, 1998).
8. H. Ma, *Plant Mol. Biol.* **26**, 1611 (1994).
9. M. Ashikari, J. Wu, M. Yano, T. Sasaki, A. Yoshimura, *Proc. Natl. Acad. Sci. U.S.A.* **96**, 10284 (1999).
10. T-DNA–tagged *Arabidopsis* mutants (60,480) (*31*) were generated at the University of Wisconsin Knockout *Arabidopsis* facility (www.biotech.wisc.edu/Arabidopsis/) and screened for insertions. Primers specific for the T-DNA left-border (5′-CATTTTATAATAACGCTGCGGACATCTAC-3′) and the T-DNA right-border (5′-TGGGAAAACCTGGCGTTACCCAACTTAAT-3′) were used in tandem with Gα-specific primers (forward: 5′-GGACCTTTCGGCGTAATTTCGTCTTCCC-3′; and reverse: 5′-CTAGTCGTAGCCATCGAGACACATTAGA-3′) for identification and isolation of the mutant lines.
11. S. R. Sprang, *Annu. Rev. Biochem.* **66**, 639 (1997).
12. A. H. Haber, *Am. J. Bot.* **49**,583 (1962).
13. A. Hemerly *et al.*, *EMBO J.* **14**, 3925 (1995).
14. A. M. Jones *et al.*, *Science* **282**, 1114 (1998).
15. E. Gendreau *et al.*, *Plant Physiol.* **114**, 295 (1997).
16. T. Tsuge, H. Tsukaya, H. Uchimiya, *Development* **122**, 1589 (1996)
17. G.-T. Kim, H. Tsukaya, Y. Saito, H. Uchimiya, *Proc. Natl. Acad. Sci. U.S.A.* **96**, 9433 (1999).
18. WS, *gpa1-1*, and *gpa1-2* seedlings were grown for 2 days in the dark on various concentrations of brassinolide (BR, 0 to 10 μM). WS and *gpa1* hypocotyl growth was inhibited by BR to 45% and 73% of the control lengths, respectively.
19. cyc1At-CDBGUS contains *Arabidopsis* cyc1At promoter and 5′ portion of the cyclin coding region fused in-frame to the reporter β-glucuronidase (GUS) gene. The fusion contains sequences encoding the cyclin destruction box (CDB). cyc1At-CDBGUS plants were crossed into *gpa1* mutant plants. *gpa1* mutants were selected from a F_2 population grown for 2 days in dark. The selected plants were allowed to grow for an additional 48 to 72 hours in light before staining. The seedlings were stained for GUS activity.
20. P. M. Donnelly, D. Bonetta, H. Tsukaya, R. E. Dengler, N. G. Dengler, *Dev. Biol.* **215**, 407 (1999).
21. T. Vernoux *et al.*, *Plant Cell* **12**, 97 (2000).
22. Supplementary data are available on *Science* Online at www.sciencemag.org/cgi/content/full/292/5524/2066/DC1.
23. G. Liebmann, F. D. Böhmer *Curr. Med. Chem.* **7**, 911 (2000).
24. M. Nishida *et al.*, *Nature* **408**, 492 (2000).
25. I. Lopez, E. C. Mak, J. Ding, H. E. Hamm, J. W. Lomasney, *J. Biol. Chem.* **276**, 2758 (2001).
26. D. G. Lambright *et al.*, *Nature* **379**, 311 (1996).
27. J. Sondek, A. Bohm, D. G. Lambright, H. E. Hamm, P. B. Sigler, *Nature* **379**, 369 (1996).
28. Y. Kovtun, W.-L. Chiu, W. Zeng, J. Sheen, *Nature* **395**, 716 (1998).
29. T. M. Jelacic, M. E. Kennedy, K. Wickman, D. E. Clapham, *J. Biol. Chem.* **275**, 36211 (2000).
30. X.-Q. Wang, H. Ullah, A. M. Jones, S. M. Assmann, *Science* **292**, 2070 (2001).
31. P. J. Krysan, J. C. Young, M. R. Sussman, *Plant Cell* **11**, 2283 (1999).
32. C. A. Weiss, E. White, H. Huang, H. Ma, *FEBS Lett.* **407**, 361 (1997).

33. We thank J. Celenza (Boston University) for the mitotic reporter (cyc1At-CDB-GUS) plants and H. Ma (Penn State University) for antiserum to GPA1 and *GPA1* cDNA. We gratefully acknowledge the support of the National Science Foundation, Integrative Plant Sciences. K.-H.I. was supported by a grant to A.M.J. from the U.S. Department of Agriculture.

16 January 2001; accepted 6 April 2001